Using Regularized Softmax Regression in the GNSS/INS Integrated Navigation System with Nonholonomic Constraints

IOP Conf. Series: Materials Science and Engineering **538** (2019) 012058 doi:10.1088/1757-899X/538/1/012058

Using Regularized Softmax Regression in the GNSS/INS Integrated Navigation System with Nonholonomic Constraints

Linlin Zhao, Haiyang Quan

Beijing Microelectronics Technology Institute, Beijing, China

Corresponding author's e-mail:elijaheslyz@buaa.edu.cn

Abstract. The integration of global navigation satellite system (GNSS) and Inertial navigation system (INS) is widely implemented in land-vehicle navigation applications. However, the satellite signal is vulnerable in some special urban scenarios, consequently errors in terms of position, velocity and attitude grow rapidly in stand-alone mode especially for low-cost MEMS-based INS. In the conventional tight combination navigation schemes, system works on predicting model during the GNSS signal outage and the positioning accuracy is determined by the precision of the inertial navigation. Besides the lack of observation makes the estimate of inertial navigation error with GNSS information less reliable due to the satellite signal loss. In this paper, an improved non-holonomic constraints (NHC) method based on regularized softmax regression is proposed to enhance navigation precision when the number of visible satellite is insufficient. The velocity constraint condition is applied to simplify the system calculating equations of MEMS-based INS. Furthermore, a regularization softmax regression model based on the collected data is trained to recognize the vehicle motion pattern so as to realize deeper constraints. Simulation and field-test results indicate that the method is beneficial to raise the precision of low-cost GNSS/INS integrated navigation receiver by efficiently reduce the navigation errors.

1. Introduction

Integrated navigation receiver-chips based on global navigation satellite system (GNSS) and Inertial navigation system (INS) have been widely applied in various fields such as land-vehicle navigation (LVN) [1]. The integration of GNSS and INS takes advantage of the both navigation methods since an INS is self-contained and able to provide full six degree-of-freedom solutions with high update rates which covers the shortage of satellite navigation on anti-jamming. Micro-electro-mechanical systems (MEMS) inertial sensors are predominant in power consumption, weight and cost which quitely meet the specifications and requirements for INS. However, the widespread uses of MEMS inertial systems that are of low-cost and low-grade inertial sensors outputs are characterized by high noise and large indeterminacy and consequently this reduction of cost has led to drop in accuracy as a whole [2-3]. Therefore, an INS that uses low-cost inertial sensors only can be used for standalone navigation for a very limited time period. Even though the system can estimate the sensor biases, the position error growth during the GNSS-signal outages is substantial and the navigation solution soon becomes useless.

Some research suggests that the navigation precision could be improved by raising hardware structure or importing other sensors data [4-6]. A preferable performance system can be realized, whereas the cost and systematic complexity increase as well. A short discussion about various information fusion

strategies is proposed in [7]. In most integrated schemes, the GNSS is considered to be an accurate reference with which to correct for the systematic errors of the inertial sensors. Admitting that an integrated navigation system can work in GNSS-denied environments, the lack of observation makes the estimate of inertial navigation error with GNSS information less reliable. It is valuable to introduce specific auxiliary information without adding extra hardware costs. For LVN applications, Non-Holonomic Constraints (NHC) is one of the most common types of auxiliary information. A detailed observability analysis of the contributions of the NHC from the perspective of observability is given in [8], which provides a deeper insight and shows how the NHC improves the navigation solutions in a loosely coupled GPS-aid INS. Niu [9] implemented the NHC in land-vehicle navigation which could significantly improve the heading accuracy. But it would barely contribute when the speed gets low. Shin [10] proposed a method to constrain the heading drift which is called Zero Integrate Heading Rate. The current approaches still need deeper constrains to cover the various situations.
In this paper, a tightly integrated navigation system with NHC based on low-cost INS and GNSS receiver is proposed. The equations of INS pseudo-range and pseudo-range rate are described in detail. The NHC condition is also imported to the combination filter for the LVN applications. Further, we implemented regularized softmax regression to recognize the vehicle motion mode so that deeper constrains could be realized. Simulation analysis verified the effectiveness of our method and field-test results showed a significant improvement on the performance during the satellite signal outage.

2. Method

2.1. Overall Design of the Tightly-Coupled Scheme

A succinct expression of the integrated navigation scheme is described in Fig.1. A relative distance to satellite that can be considered as the pseudo-range and pseudo-range rate of INS is calculated with the inertial navigation outcome and the satellite ephemeris information. The pseudo-range and pseudo-range rate offset between GNSS measurement and INS are implemented as the input factors of the extended Kalman filter [11]. It is mentioned that data pre-processing and initial alignment steps are not involved in the discussion of this paper which cannot be considered as vacancy.

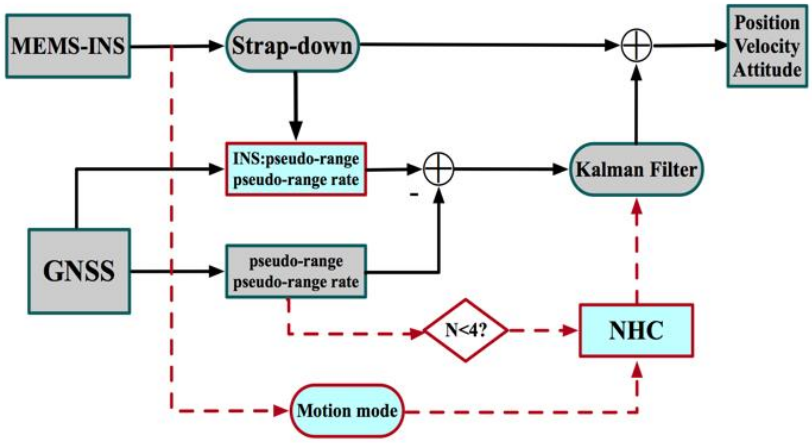

Figure1. The overall scheme of GNSS/INS

A 11-state vector which updates by the tightly-coupled INS/GNSS integrated filter based on the pseudo-range and pseudo-range rate is defined in (1).

$$X = [\phi_e \ \phi_n \ \phi_u \ \Delta\lambda \ \Delta l \ \Delta h \ \Delta v_e \ \Delta v_n \ \Delta v_u \ \delta t_u \ \delta t_{ru}]^T \tag{1}$$

Where the subscripts *e, n* and *u* represent the three axis of geocentric coordinate system and λ, *l and h* represent the position of longitude, latitude and altitude. ϕ represents error-angle of platform and errors of velocity, clock and frequency are considered as Δv, δt_u and δt_{ru}.

2.2. Equations of pseudo-range and pseudo-range rate

The position measurement from INS can be assumed as $(\boldsymbol{x_I\ y_I\ z_I})^{\boldsymbol{T}}$and accurate satellite position can be extracted from the ephemeris information as $(\boldsymbol{x_s\ y_s\ z_s})^{\boldsymbol{T}}$. The pseudo-range measurement from GNSS receiver is defined as $\boldsymbol{\rho_G}$. The real distance from INS to GNSS satellites can be described as (2).

$$r_j = \left[\left(x_{sj} - x\right)^2 + \left(y_{sj} - y\right)^2 + \left(z_{sj} - z\right)^2\right]^{\frac{1}{2}} \tag{2}$$

The factual coordinate orientation is set as $(\mathrm{x\ y\ z})^{\mathrm{T}}$and Taylor series expansion in the measurement from INS can be defined as (3) and the first order is reserved. Therefore, we can express the pseudo-range with position error and $\mathrm{r_j}$ as (5).

$$r_j = \left[\left(x_{sj} - x_I\right)^2 + \left(y_{sj} - y_I\right)^2 + \left(z_{sj} - z_I\right)^2\right]^{\frac{1}{2}} - H \tag{3}$$

$$H = \frac{\partial r_j}{\partial x}\delta x + \frac{\partial r_j}{\partial y}\delta y + \frac{\partial r_j}{\partial z}\delta z \tag{4}$$

$$\rho_{Ij} = r_j - e_{j1}\delta x - e_{j2}\delta y - e_{j3}\delta z \tag{5}$$

$$\frac{\partial \rho_j}{\partial x} = -\frac{x_{sj} - x_I}{r_j} = -e_{j1} \tag{6}$$

$$\frac{\partial \rho_j}{\partial y} = -\frac{y_{sj} - y_I}{r_j} = -e_{j2} \tag{7}$$

$$\frac{\partial \rho_j}{\partial z} = -\frac{z_{sj} - y_I}{r_j} = -e_{j2} \tag{8}$$

Similarly, we can infer the expression of the pseudo-range rate as (11). Prior to that the expressions of pseudo-range and pseudo-range rate from GNSS receiver are given in (9) and (10). $\upsilon_{\rho j}$ stands for the ionospheric errors of satellite *j*.

$$\rho_{Gj} = r_j + \delta t_u + \upsilon_{\rho j} \tag{9}$$

$$\dot{\rho}_{Gj} = e_{j1}\left(\dot{x}_{sj} - \dot{x}\right) + e_{j2}\left(\dot{y}_{sj} - \dot{y}\right) + e_{j3}\left(\dot{z}_{sj} - \dot{z}\right) + \delta t_{ru} + \dot{\upsilon}_{\rho j} \tag{10}$$

$$\dot{\rho}_{Ij} = \dot{r}_j - e_{j1}\delta \dot{\mathrm{x}} - e_{j2}\delta \dot{y} - e_{j3}\delta \dot{z} \tag{11}$$

The measurement equations of the pseudo-range and pseudo-range rate offset can eventually be expressed as follows.

$$\delta\rho_j = e_{j1}\delta x + e_{j2}\delta y + e_{j3}\delta z + \delta t_u + \upsilon_{\rho j} \tag{12}$$

$$\delta\dot{\rho}_j = e_{j1}\delta \dot{x} + e_{j2}\delta \dot{y} + e_{j3}\delta \dot{z} + \delta t_{ru} + \dot{\upsilon}_{\rho j} \tag{13}$$

The tightly-coupled integrated system then takes the pseudo-range and pseudo-range rate offset as observed quantity of the combination filter to update the navigation information.

2.3. The Non-Holonomic Costraints for LVN

When the number of visible satellites is less than four, although the combination filter still works, poor navigation results are given due to the lack of measurement. The NHC method is actually used commonly in the navigation of land vehicles [9]. For land vehicles in urban environment, it can be assumed that the height of carrier will not abruptly change in a short time. Thus, the height before it lost a moment can be used as a constraint in the process of GNSS disruption. Besides the NHC makes assumptions that in the case of LVN, the velocity of the vehicle in the plane perpendicular to the forward direction is almost zero unless the vehicle jumps off the ground or slides on the ground. The velocity constraint can be expressed as (14).

$$\left(v_x^b, v_z^b\right)^T \sim N(0, R_v) \tag{14}$$

where R_v stands for the perturbation error due to the angle misalignment. For the height constraint, a measurement equation is imported to the system as shown in (15).

$$h_{INS} - h_{const} = \delta h + v \tag{15}$$

Where h_{INS} and h_{const} represent the current solution of INS and previous solution of GNSS in height. If h_{const} is of highly authenticity, the navigation solution is equal to the normal mode. Otherwise the measured values have a deviation of the system. In accordance with the standard Kalman filtering equation, the measurement deviation will be imported the state estimation equation to influence the filtering solution, the height constraint can cause larger error when h_{const} is unreliable. However, for land vehicle system, height will not cause large-scale fluctuations and even assuming that the height is not accurate anyway, the positioning solutions are still better than that of without constraints. When it comes to the velocity constraints, it is equivalent to add another two assumed truth values. Similar to the height constraint, if the vehicle is in high dynamic circumstances, such as making a turn or greatly changing directions, the estimation error could be worse. Therefore, deeper constraints are still in need for the NHC method.

3. Improved Method on Deeper Constraints

3.1. Reguarized Softmax Regression in Motion Mode Recognition

As is mentioned that constraints of position and velocity are not reliable when the vehicle changes attitude or directions. In other word, the performance of NHC is affected by the motion state. Inertial sensors can reflect the movement of the carrier which can determine the current motion state to import different constraint conditions according to the output of INS.

Softmax regression is an extension for logistic regression on the multiple classification problems [12] which is a kind of real-time supervised learning model. The softmax function and loss function are defined as follows.

$$h_\theta\left(x^{(i)}\right) = \frac{1}{\sum_{j=1}^{3} exp\left(\boldsymbol{\theta}_j^T \boldsymbol{x}^{(i)}\right)} \begin{bmatrix} exp\left(\boldsymbol{\theta}_1^T \boldsymbol{x}^{(i)}\right) \\ exp\left(\boldsymbol{\theta}_2^T \boldsymbol{x}^{(i)}\right) \\ exp\left(\boldsymbol{\theta}_3^T \boldsymbol{x}^{(i)}\right) \end{bmatrix} \tag{16}$$

$$\boldsymbol{J(\theta)} = -\frac{\mathbf{1}}{\boldsymbol{m}}\left[\sum_{i=1}^{m}\sum_{j=1}^{3}\{\boldsymbol{y}^{(i)} = \mathbf{j}\}\boldsymbol{ln}\left(\frac{\boldsymbol{exp}(\boldsymbol{\theta}_j^T \boldsymbol{x}^{(i)})}{\sum_{n=1}^{3} \boldsymbol{exp}(\boldsymbol{\theta}_n^T \boldsymbol{x}^{(i)})}\right)\right] + \boldsymbol{\lambda}\|\boldsymbol{\theta}\|^2 \tag{17}$$

Where m stands for the quality of data samples and $\boldsymbol{\theta}$ is the weighting parameter vector. Besides we imported $\lambda\|\boldsymbol{\theta}\|^2$as the regulation term to avoid parameter redundancy and overfitting. Therefore, the loss function is composed of cross entropy and regularization and iteration methods [12] can be applied to obtain the optimal solution. For vehicles, general motion states can be summarized as static, going straight and turning. A training method based on the actual data is given as Fig.2.

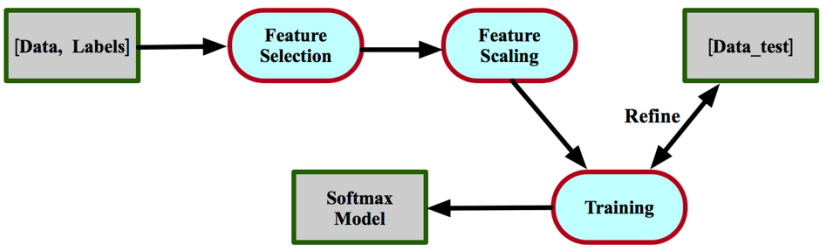

Figure 2. Training method

The data samples and calibration are generated from real road collections. Since MEMS-INS is fixed on the vehicles, the perturbation could form acceleration in the vertical direction in the process of driving. Considering the motion characteristics of land vehicles, a practical method of feature selection is proposed here. The expressions of feature are shown as follows.

$$x_1 = \sum_{t_i=t_k-n}^{t_k} \omega_{norm}\,(t_i) \tag{18}$$

$$x_2 = \sum_{t_i=t_k-n}^{t_k} |a_{norm}(t_i) - a_{norm}(t_i - i)| \tag{19}$$

$$x_3 = \frac{1}{m}\sum_{t_i=t_k-m}^{t_k} \omega_z\,(t_i) \tag{20}$$

where $\omega_{norm} = \sqrt{{\omega_x}^2 + {\omega_y}^2}$ represents the horizontal angular velocity and $a_{norm} = \sqrt{a_x^{b\,2} + a_y^{b\,2} + a_z^{b\,2}}$ stands for the total acceleration. It is noted that scale normalization is essential in the feature scaling. The range of features is unified to [0, 1]. We can get the motion state probability by softmax regression based on the current feature vector as shown in Fig.3.

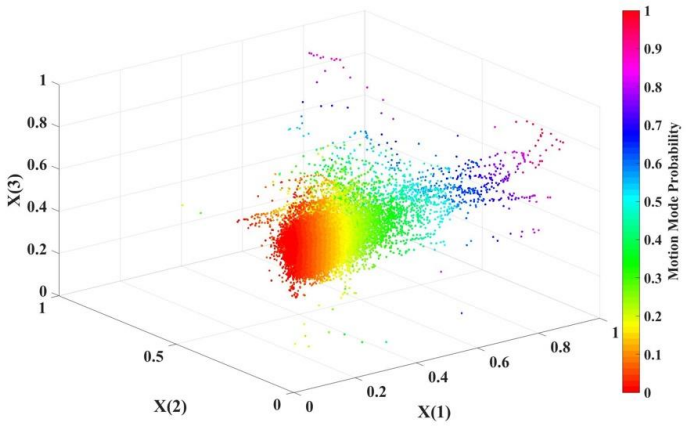

Figure 3. The probability distribution by regularized softmax regression

The motion state can be determined by the optimal probability estimate. The recognition performance in a real-road test is shown in Fig.4. The outcomes are consistent with the real motion state in most cases.

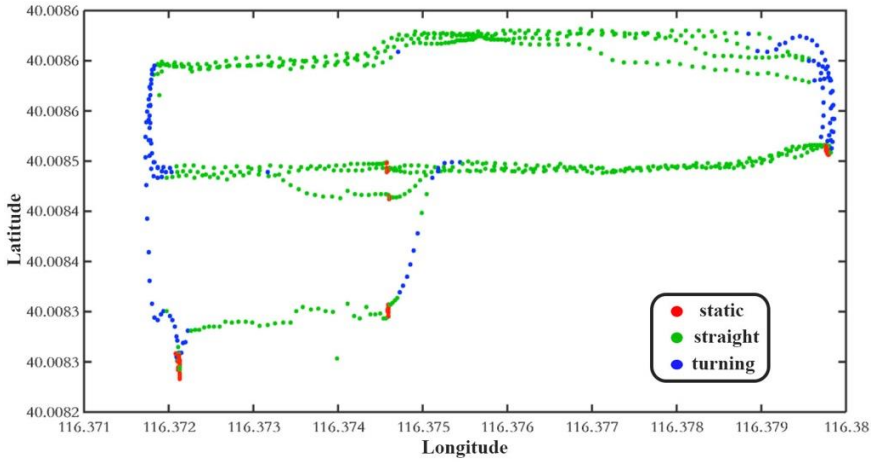

Figure 4. The motion mode solution by regularized softmax regression

3.2. Deeper Constraints for NHC

After motion mode judgement, different conditions can be derived as deeper constraints. First of all, for the static state, we need to make zero velocity update and modify the pitch and the roll by the accelerometer calibration, besides the course angle should remain and the gyroscope zero bias need recalculated. The constraints can be described as follows.

$$\boldsymbol{v} = 0 \tag{21}$$

$$\theta = \sin^{-1}\left(\frac{a_y}{g}\right) \tag{22}$$

$$\emptyset = \sin^{-1}\left(\frac{-a_x}{\sqrt{g^2 - a_y^2}}\right) \tag{23}$$

$$B_\omega = \omega \tag{24}$$

For a linear motion, the roll can be corrected by the accelerometer of x-axis which is shown in (25). As for turning mode, the velocity can be obtained by the relationship between the centripetal acceleration and the angular velocity as (26).

$$\emptyset = \sin^{-1}\left(\frac{-a_x}{\sqrt{g\cos\theta}}\right) \tag{25}$$

$$v = \frac{a_x + g\sin\phi cos\theta}{\omega_z} \tag{26}$$

4. Experiments and Discuss

4.1. Simulation of the GNSS/INS with Improved NHC

We have showed the performance of our method on the vehicle movement state recognition. Further, we imported the NHC model with regularized softmax regression to a self-developed GNSS/INS integrated navigation receiver as shown in fig.5.

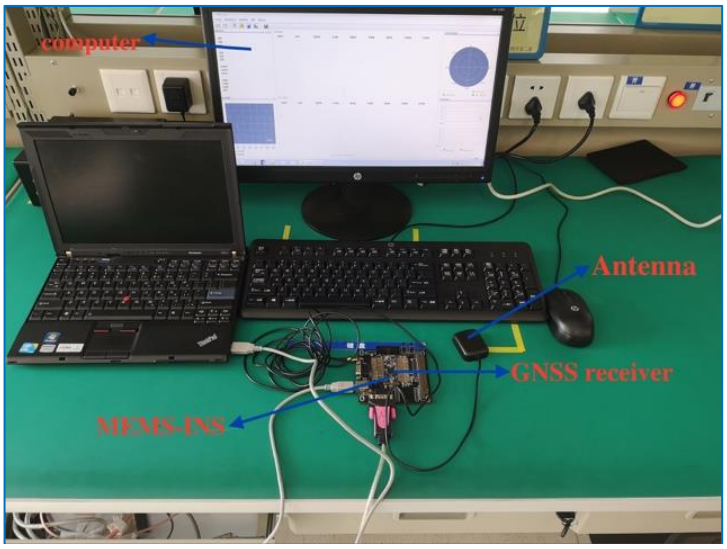

Figure 5. The self-developed GNSS/INS

The simulated environment of insufficient visible satellites is generated by the signal simulator. When the number of visible satellites is less than four, the system can still work at an excellent precision based on the improved NHC. Fig.7 shows the result error of static simulation.

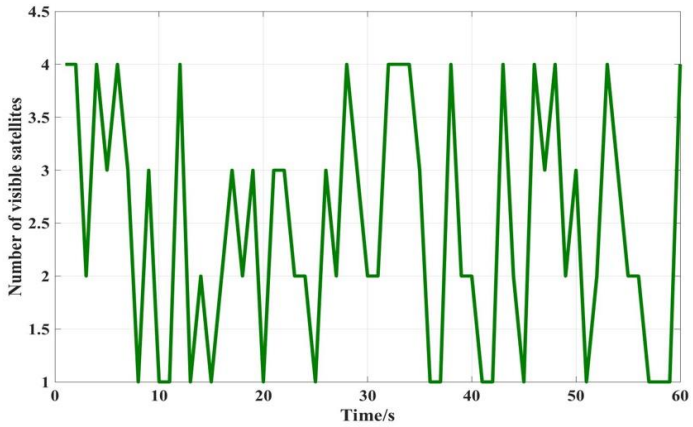

Figure 6. The number of visible satellites

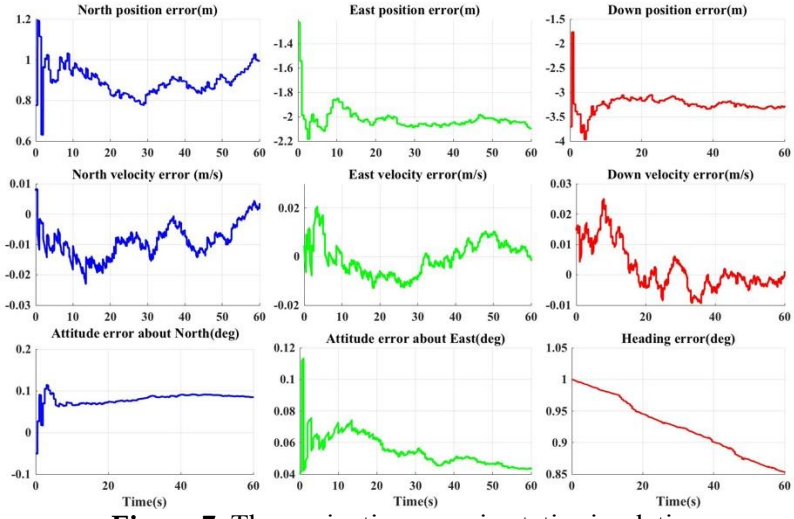

Figure 7. The navigation error in static simulation

Table1. RMSE of location error

RMSE of location error	Static Simulation
East position (m)	2.87
North position (m)	0.95
Down position (m)	3.37
East velocity (m/s)	0.02
North velocity (m/s)	0.01
Down velocity (m/s)	0.12
Pitch (°)	0.18
Roll (°)	0.12

Splendid performance of error limitation could be realized by our method in the static simulation as shown in table 1. It's understandable that the improvement on precision is produced by NHC. The system will work at zero-velocity updating mode once it is recognized as static.

4.2. Field-test Experiment

A field-test is conducted along the route shown in Fig.8 which is composed of general urban scenario. We measured the navigation errors as well and performance of the method can be seen in Fig.9.

Figure 8. The road-test route

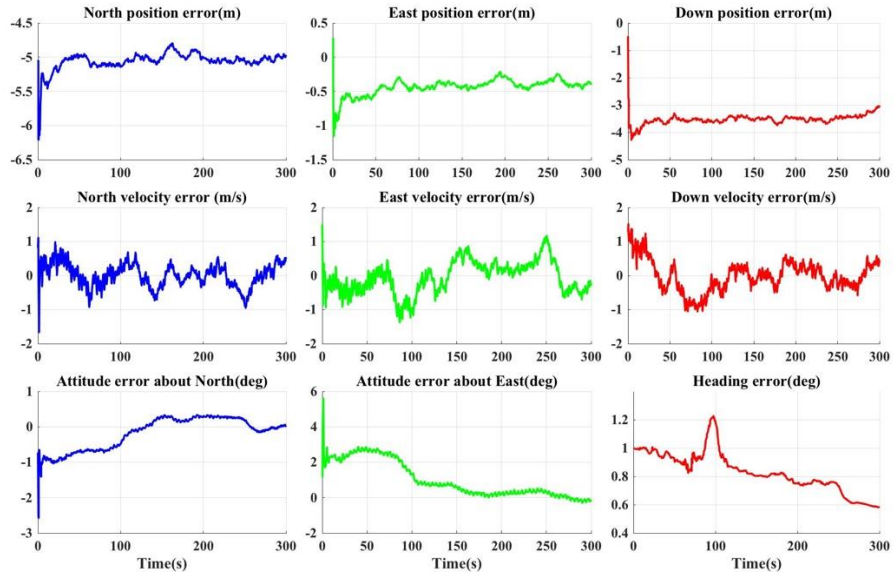

Figure 9. The navigation error of road test

Table2. RMSE of location error

RMSE of location error	Static Simulation
East position (m)	5.47
North position (m)	0.75
Down position (m)	3.89
East velocity (m/s)	0.98
North velocity (m/s)	1.12
Down velocity (m/s)	0.87
Pitch (°)	1.12
Roll (°)	1.84

As is shown in Fig.9 and table 2, since the practical test is complex, the navigation error is worse than static simulation but still proves an acceptable precision. Besides, the down position error is caused by the initial alignment. For low-end MEMS based navigation system in LVN applications, we improved the navigation performance by using the regularized softmax regression in NHC to realize deeper constraints and the effectiveness has been verified.

5. Conclusion

In this paper, we successfully implemented regularized softmax regression into a self-developed tightly integrated navigation system with NHC based on a low-cost INS and GNSS receiver. The regularized softmax regression is applied to recognize the vehicle motion mode so that deeper constrains could be realized. Detailed analysis and field-test results inferred that our method could significantly raise the performance of the system especially during the GNSS outage.

Acknowledgments

This study was partially supported by the College specialized research project from Beihang University and the navigation research center of Beijing Microelectronics Technology Institute.

References

[1] Aboelmagd Noureldin, Tashfeen B Karamat, and Jacques Georgy. Funda- mentals of Inertial Navigation, Satellite-Based Positioning and Their Inte- gration. Springer, 2013.

[2] E. H. Shin and N. El-Sheimy, “Accuracy improvement of low cost INS/GPS for land applications,” Department of Geomatics Engineering, University of Calgary, 2001.

[3] E. H. Shin, “Estimation techniques for low-cost inertial navigation,” UCGE report, 2005.

[4] Y. Tawk, P. Tome, and C. Botteron, “Implementation and Performance of a GPS/INS Tightly Coupled Assisted PLL Architecture Using MEMS Inertial Sensors,” *Sensors* 2014, 14, 3768-3796.

[5] Yang, Y. “Tightly Coupled MEMS INS/GPS Integration with INS Aided Receiver Tracking Loops,” University of Calgary: Calgary, AB, Canada, 2008.

[6] Niu, X., Hassan, T., Ellum C., and El-Sheimy, N., 2006. Directly Georeferencing Terrestrial Imagery using MEMS- based INS/GNSS Integrated Systems. In: *XXIII FIG (International Federation of Surveyors) Congress*, Munich, Germany, 8-13 October 2006. .

[7] Isaac Skog and Peter Handel, “In-car Positioning and Navigation Technologies—A Survey,” IEEE transactions on Intelligent Transportation systems, VOL. 10, NO. 1, March 2009.

[8] X. Niu, Y. Li, Q. Zhang, Y. Cheng and Ch. Shi, “Observability Analysis of Non-Holonomic Constraints for Land-Vehicle Navigation Systems,” Journal of Global Positioning Systems, Vol.11, No.1 : 80-88, 2012.

[9] X. Niu, S. Nassar, and N. El-Sheimy, “An accurate land-vehicle MEMS IMU/GPS navigation system using 3D auxiliary velocity updates,” *Navigation, Journal of the Institute of Navigation*, vol. 54, no. 3, pp. 177–188, 2007.

[10] Shin, E. H., 2005. Estimation Techniques for Low-Cost Inertial Navigation. PhD Thesis, MMSS Research Group, Department of Geomatics Engineering, University of Calgary, Calgary, AB, Canada, UCGE Report No. 20219.

[11] Shin, E. H., 2005. Estimation Techniques for Low-Cost Inertial Navigation. PhD Thesis, MMSS Research Group, Department of Geomatics Engineering, University of Calgary, Calgary, AB, Canada, UCGE Report No. 20219.

[12] Pereira F., Mitchell T. and Botvinick M., Machine Learning Classifiers and fMRI: A Tutorial Overview. NeuroImage, 2009, 45(1): S199-S209